
Neural Likelihoods for Multi-Output Gaussian Processes

Martin Jankowiak*
Uber AI Labs
San Francisco, CA, USA

Jacob Gardner
Uber AI Labs
San Francisco, CA, USA

Abstract

We construct flexible likelihoods for multi-output Gaussian process models that leverage neural networks as components. We make use of sparse variational inference methods to enable scalable approximate inference for the resulting class of models. An attractive feature of these models is that they can admit analytic predictive means even when the likelihood is non-linear and the predictive distributions are non-Gaussian. We validate the modeling potential of these models in a variety of experiments in both the supervised and unsupervised setting. We demonstrate that the flexibility of these ‘neural’ likelihoods can improve prediction quality as compared to simpler Gaussian process models and that neural likelihoods can be readily combined with a variety of underlying Gaussian process models, including deep Gaussian processes.

1 Introduction

Significant effort has gone into developing flexible, tractable probabilistic models, especially for the supervised settings of regression and classification. These include, among others, multi-task Gaussian processes (Bonilla et al., 2008), Gaussian process regression networks (Wilson et al., 2011), deep Gaussian processes (Damianou and Lawrence, 2013), Gaussian processes with deep kernels (Wilson et al., 2016; Calandra et al., 2016), as well as various approaches to Bayesian neural networks (Graves, 2011; Blundell et al., 2015; Hernández-Lobato and Adams, 2015). While neural networks promise considerable flexibility, scalable learning

algorithms for Bayesian neural networks that can deliver robust uncertainty estimates remain elusive.

For this reason Gaussian processes (GPs) are an important class of models in cases where predictive uncertainty estimates are important. Gaussian processes offer several key advantages over other probabilistic models:¹ i) the covariance functions they employ typically have a semantic meaning that is natural for practitioners to reason about; ii) they facilitate incorporating prior knowledge; and iii) they tend to yield high-quality uncertainty estimates, even for out-of-sample data. These strengths mirror corresponding weaknesses of current approaches to Bayesian neural networks, weaknesses that become especially evident in the small data regime, where Bayesian neural networks often struggle to deliver meaningful uncertainties. Despite these strengths, the simplest variants of GP models often fall short of the flexibility of their neural network counterparts.

In recent years, a number of researchers have formulated more flexible Gaussian process models by modifying the GP prior itself. One approach has been to define richer classes of kernels. This approach is exemplified by deep kernels, which use a deep neural network to define a rich parametric family of kernels (Wilson et al., 2016; Calandra et al., 2016). Another complementary approach is the use of deep Gaussian processes, which compose multiple layers of latent functions to build up more flexible—in particular non-Gaussian—function priors (Damianou and Lawrence, 2013). Surprisingly little attention, however, has been paid to the flexibility of *likelihoods* in this setting. This is likely because, historically, the likelihoods used in the multi-output setting have often been constrained for computational reasons. However, with recent advances in stochastic gradient methods, some of these structural assumptions are no longer required to enable efficient inference.

¹We refer the reader to (Rasmussen, 2003) for a general introduction to GPs.

*Correspondence to: jankowiak@uber.com

With this opportunity in mind, our aim in this work is to make multi-output Gaussian process models more flexible by equipping them with more flexible likelihoods. We employ two simple modeling patterns to construct richer likelihoods. To make these modeling patterns more concrete, let $\mathbf{F}(\mathbf{x})$ denote the latent vector of function values drawn from a multi-output GP prior evaluated at an input \mathbf{x} . In the first approach, we pass $\mathbf{F}(\mathbf{x})$ through what is in effect a single-layer neural network before adding Gaussian observation noise. Alternatively, in a second approach we multiply $\mathbf{F}(\mathbf{x})$ by a matrix of coefficients controlled by a deterministic neural network that depends on the inputs to the GP. This latter approach—which can be viewed as a semi-Bayesian version of the Gaussian Process Regression Network (Wilson et al., 2011)—is more flexible but is potentially more prone to overfitting.

We find that both modeling patterns result in flexible models that admit efficient inference using sparse variational methods. Furthermore, we demonstrate empirically that this added flexibility can lead to considerable gains in predictive performance. Importantly, these *neural* likelihoods are complementary to other approaches for making GP models more flexible, including, for example, deep Gaussian processes and deep kernels.

The rest of this paper is organized as follows. In Sec. 2 we place our work in the context of related work. In Sec. 3 we describe the models with neural likelihoods that are the focus of this work. In Sec. 4 we describe scalable inference algorithms for this class of models. In Sec. 5 we demonstrate the modeling potential of neural likelihoods with a series of experiments.

2 Related Work

As discussed in the introduction, a large body of work aims to make GP priors more flexible, including deep Gaussian processes (Damianou and Lawrence, 2013), GPs with deep kernels (Wilson et al., 2016; Calandra et al., 2016), recurrent Gaussian processes (Mantos et al., 2015), spectral mixture kernels (Wilson and Adams, 2013), and compositional kernels (Sun et al., 2018). In the same spirit, a variety of GP models have been proposed that model correlations between multiple outputs (Alvarez and Lawrence, 2009; Álvarez and Lawrence, 2011). In particular these include a number of models that have been formulated in the multi-task setting (Bonilla et al., 2008; Williams et al., 2009; Nguyen et al., 2014), including models for Bayesian optimization (Swersky et al., 2013). As mentioned in the introduction, much of this work makes particular structural assumptions about the covariance structure and/or likelihood for computational convenience; this limits the flexibility of

these models. In this context see (Dezfooli and Bonilla, 2015) for an application of sparse variational methods to a broader class of likelihoods. Finally, Snelson et al. (2004) construct flexible likelihoods in the GP setting by warping the observed outputs with a learned deterministic bijection.² A similar model, where the warping function is modeled by a GP, is considered in (Lázaro-Gredilla, 2012). Our N-MOGP model is closest to this latter setup, with the difference that we work in the multi-output setting and our warping function is provided by a Bayesian neural network.

A number of researchers have explored models that combine various aspects of GPs and neural networks. For example, Cutajar et al. (2017) use random feature expansions to formulate a link between deep GPs and Bayesian neural networks that then enables efficient inference in the resulting class of models. In (Ma et al., 2018), the authors propose implicit stochastic processes as a framework for defining flexible function priors; similarly, Neural Processes are a recent class of models that combine aspects of stochastic processes with neural networks (Garnelo et al., 2018a,b). Both these classes of models generally do not employ explicit kernel functions as is characteristic of GPs. Finally, another work with close analogs to deep kernels is (Huang et al., 2015).

3 Models

In this section we define the class of models that is the focus of this work. First, in Sec. 3.1 we equip Gaussian process regression models with neural likelihoods. Next, in Sec. 3.2 we repurpose a subset of the same models for the unsupervised setting.

Throughout we use the following notation. In the regression setting we suppose we are given a dataset $\mathcal{D} = \{(\mathbf{x}_i, \mathbf{y}_i)\}_{i=1}^N$ of size N with each input $\mathbf{x}_i \in \mathbb{R}^{D_x}$ and each output $\mathbf{y}_i \in \mathbb{R}^{D_y}$. We use \mathbf{X} and \mathbf{Y} to refer to the full set of inputs and outputs, respectively. In the unsupervised setting we assume a dataset $\mathcal{D} = \{\mathbf{y}_i\}_{i=1}^N$.

3.1 Models for Regression

In Sec. 3.1.1-3.1.3 we specify three baseline GP models. Then in Sec. 3.1.4-3.1.7 we modify and/or extend these baseline models to obtain four models with neural likelihoods that will form the basis of our experiments.

²We experimented with similar constructions but found them to perform poorly in the multi-output setting, suffering from a tendency to get stuck in bad local optima.

3.1.1 Multi-Output Gaussian Processes

We begin by defining our simplest baseline model, a basic multi-output Gaussian process (**MOGP**).³ We define L independent Gaussian processes $\{\mathbf{f}_\ell(\mathbf{x})\}$ with $\ell = 1, \dots, L$ and each with kernel K_ℓ .⁴ For a given input \mathbf{x} we use $\mathbf{F}(\mathbf{x})$ to denote the L -dimensional latent vector of GP function values at \mathbf{x} . The marginal probability of the MOGP is then specified as follows

$$p(\mathbf{Y}|\mathbf{X}) = \int d\mathbf{M} p(\mathbf{M}) \prod_{\ell=1}^L d\mathbf{f}_\ell p(\mathbf{f}_\ell|\mathbf{X}) \times \prod_{i=1}^N \mathcal{N}(\mathbf{y}_i | \mathbf{M}\mathbf{F}(\mathbf{x}_i), \boldsymbol{\beta}) \quad (1)$$

where \mathbf{M} is a $D_Y \times L$ mixing matrix, $\mathbf{M}\mathbf{F}$ denotes matrix multiplication, and $p(\mathbf{M})$ is a unit Normal prior on \mathbf{M} . Here and throughout $\boldsymbol{\beta}$ is a D_Y -dimensional vector of precisions that controls the (diagonal) observation noise

Note that for fixed \mathbf{M} the covariance structure of the D_Y -dimensional vector $\mathbf{M}\mathbf{F}(\mathbf{x})$ is that of the ‘linear model of coregionalization’ (LMC) (Alvarez et al., 2012). While other covariance structures for the Gaussian process prior are possible, for uniformity—and since our primary interest is to investigate modifications to the likelihood—all our models employ this basic pattern. For the same reason we use RBF kernels throughout.

3.1.2 Gaussian Process Regression Networks

A natural generalization of the model in Eqn. 1 is the Gaussian Process Regression Network (**GPRN**) (Wilson et al., 2011). In effect we promote \mathbf{M} to a \mathbf{x} -dependent matrix of Gaussian processes to obtain a model

$$P(\mathbf{Y}|\mathbf{X}) = \int \prod_{\ell=1}^L d\mathbf{f}_\ell p(\mathbf{f}_\ell|\mathbf{X}) \prod_{m_\ell=1}^{D_Y} d\mathbf{m}_{m_\ell} p(\mathbf{m}_{m_\ell}|\mathbf{X}) \times \prod_{i=1}^N \mathcal{N}(\mathbf{y}_i | \mathbf{M}(\mathbf{x}_i)\mathbf{F}(\mathbf{x}_i), \boldsymbol{\beta}) \quad (2)$$

where $\mathbf{M}(\mathbf{x}_i)$ is now a $D_Y \times L$ random variable governed by a GP prior.⁵ Note that this model utilizes $(D_Y + 1) \times L$ Gaussian processes and so we generally expect inference to be expensive for this class of models.

³Compare to the model in (Seeger et al., 2005).

⁴In general we assume that each K_ℓ has its own kernel hyperparameters; we specify when this is not the case.

⁵Following (Wilson et al., 2011) we share kernel hyperparameters among the Gaussian processes $\{\mathbf{m}_{m_\ell}\}$ but maintain individual kernels for the L Gaussian processes $\{\mathbf{f}_\ell\}$. In addition each kernel K_ℓ for the latent function \mathbf{f}_ℓ includes a diagonal noise component.

3.1.3 Two Layer Deep Gaussian Processes

We consider a deep multi-output GP with two layers of latent functions (Damianou and Lawrence, 2013)

$$P(\mathbf{Y}|\mathbf{X}) = \int d\mathbf{M} p(\mathbf{M}) \prod_{\ell=1}^L d\mathbf{f}_\ell p(\mathbf{f}_\ell|\mathbf{X}) \prod_{\ell'=1}^{L'} d\tilde{\mathbf{f}}_{\ell'} p(\tilde{\mathbf{f}}_{\ell'}|\mathbf{f}_{1:L}) \times \prod_{i=1}^N \mathcal{N}(\mathbf{y}_i | \mathbf{M}\tilde{\mathbf{F}}(\mathbf{x}_i), \boldsymbol{\beta}) \quad (3)$$

where $\tilde{\mathbf{F}}(\mathbf{x})$ is the L' -dimensional vector of Gaussian process function values at \mathbf{x} . Here \mathbf{M} is a $D_Y \times L'$ matrix and $p(\mathbf{M})$ denotes a unit Normal prior.⁶ We refer to this model as **DGP**.

3.1.4 Semi-Bayesian Gaussian Process Regression Networks

We now introduce the first model of interest in this work, namely a semi-Bayesian variant of the model specified by Eqn. 2. We simply ‘demote’ $\mathbf{M}(\mathbf{x}_i)$ in Eqn. 2 to a (deterministic) neural network:⁷

$$P(\mathbf{Y}|\mathbf{X}) = \int \prod_{\ell=1}^L d\mathbf{f}_\ell p(\mathbf{f}_\ell|\mathbf{X}) \prod_{i=1}^N \mathcal{N}(\mathbf{y}_i | \mathbf{M}(\mathbf{x}_i)\mathbf{F}(\mathbf{x}_i), \boldsymbol{\beta}) \quad (4)$$

Below we refer to this model as **SBGPRN**; it can be viewed as occupying an intermediate position between the MOGP and GPRN.

3.1.5 Neural Multi-Output Gaussian Processes

A natural extension to the MOGP specified by Eqn. 1 is to pass the vector of Gaussian processes \mathbf{F} through a layer of non-linearities before using \mathbf{F} to compute a mean function for the likelihood, i.e. we consider a model specified by its marginal likelihood as

$$\int d\mathbf{M} p(\mathbf{M}) \prod_{\ell=1}^L d\mathbf{f}_\ell p(\mathbf{f}_\ell|\mathbf{X}) \prod_{i=1}^N \mathcal{N}(\mathbf{y}_i | \mathbf{M}\sigma(\tilde{\mathbf{M}}\mathbf{F}(\mathbf{x}_i)), \boldsymbol{\beta}) \quad (5)$$

⁶Another alternative would be to choose $L' = D_Y$ and set $\mathbf{M} \rightarrow \mathbf{1}$. Since, however, we are particularly interested in the regime where D_Y could be quite high-dimensional—and because inference quickly becomes expensive for this class of models as we increase L and L' —we would like to avoid deep GP models with a very large number of latent functions.

⁷For simplicity we regularize the neural network $\mathbf{M}(\mathbf{x})$ with L2-regularization on the weights, although other schemes are possible as well.

where $\widetilde{\mathbf{M}}$ is a $D_H \times D_L$ matrix⁸ and \mathbf{M} is a $D_Y \times D_H$ matrix, where D_H is a new hyperparameter that controls the number of ‘hidden units.’ Here $\sigma(\cdot)$ is a fixed point-wise non-linearity (e.g. ReLU) and we place a unit Normal prior on \mathbf{M} . Below we refer to this model as **N-MOGP**. Since this model does not contain a (deterministic) neural network conditioned on the inputs as a subcomponent, we generally expect it to be less susceptible to overfitting than the SBGPRN. Note that, as is commonly done in the case of neural networks, we include a (stochastic) bias for each of the D_H hidden units; see the supplementary materials for details.

3.1.6 Neural Semi-Bayesian Gaussian Process Regression Networks

In analogy to the Neural MOGP, a natural extension to the SBGPRN is to pass the vector of Gaussian processes \mathbf{F} through a layer of non-linearities before applying the mixing matrix $\mathbf{M}(\mathbf{x})$, yielding a model specified via its marginal probability as

$$\int \prod_{\ell=1}^L d\mathbf{f}_\ell p(\mathbf{f}_\ell | \mathbf{X}) \prod_{i=1}^N \mathcal{N}(\mathbf{y}_i | \mathbf{M}(\mathbf{x}_i) \sigma(\widetilde{\mathbf{M}}\mathbf{F}(\mathbf{x}_i)), \beta) \quad (6)$$

Here $\sigma(\cdot)$ is a fixed non-linearity, $\widetilde{\mathbf{M}}$ is a $D_H \times L$ matrix and $\mathbf{M}(\mathbf{x})$ denotes a $D_Y \times D_H$ matrix controlled by a neural network. Here, again, D_H is a hyperparameter that controls the number of ‘hidden units.’ Below we refer to this model as **N-SBGPRN**.

3.1.7 Neural Deep Gaussian Processes

We equip the deep Gaussian process in Sec. 3.1.3 with a neural likelihood:

$$P(\mathbf{Y} | \mathbf{X}) = \int d\mathbf{M} p(\mathbf{M}) \prod_{\ell=1}^L d\mathbf{f}_\ell p(\mathbf{f}_\ell | \mathbf{X}) \prod_{\ell'=1}^{L'} d\tilde{\mathbf{f}}_{\ell'} p(\tilde{\mathbf{f}}_{\ell'} | \mathbf{f}_{1:L}) \prod_{i=1}^N \mathcal{N}(\mathbf{y}_i | \mathbf{M} \sigma(\widetilde{\mathbf{M}}\tilde{\mathbf{F}}(\mathbf{x}_i)), \beta) \quad (7)$$

where $\widetilde{\mathbf{M}}$ and \mathbf{M} are $D_H \times L'$ and $D_Y \times D_H$ -sized matrices, respectively. As above $p(\mathbf{M})$ denotes a unit Normal prior. We refer to this model as **N-DGP**.

3.2 Models with Latent Inputs

Each of the models in Sec. 3.1.1-3.1.7 can be repurposed as a model with latent inputs by adding a prior on \mathbf{X} . For

⁸Throughout we treat $\widetilde{\mathbf{M}}$ as a learnable parameter that is regularized via L2-regularization, i.e. we place a Normal prior on $\widetilde{\mathbf{M}}$ and perform MAP estimation on it.

example, for the MOGP in Sec. 3.1.1 we have

$$p(\mathbf{Y}) = \int d\mathbf{X} d\mathbf{M} p(\mathbf{X}) p(\mathbf{M}) \prod_{\ell=1}^L d\mathbf{f}_\ell p(\mathbf{f}_\ell | \mathbf{X}) \times \prod_{i=1}^N \mathcal{N}(\mathbf{y}_i | \mathbf{M}\mathbf{F}(\mathbf{x}_i), \beta) \quad (8)$$

where $p(\mathbf{X})$ is a unit Normal prior on the inputs. We investigate a subset of these models empirically in Sec. 5.4.

4 Inference

In this section we describe how we perform approximate inference for the models described in Sec. 3. In all cases we make use of variational inference due to its favorable computational properties and because it enables data subsampling during training.

4.1 Sparse Variational Methods

In order to scale inference to large datasets we make use of sparse variational methods for Gaussian processes, which we now briefly review (Titsias, 2009; Hensman et al., 2013). For every GP we introduce inducing variables \mathbf{u} with $\dim(\mathbf{u}) = N_{\text{ind}}$, which are conditioned on N_{ind} variational parameters $\{\mathbf{z}_k\}$,⁹ with each \mathbf{z}_k of the same dimension as the inputs to the GP. We then augment the GP prior with the inducing variables \mathbf{u}

$$p(\mathbf{f} | \mathbf{X}) \rightarrow p(\mathbf{f} | \mathbf{u}, \mathbf{X}, \mathbf{Z}) p(\mathbf{u} | \mathbf{Z})$$

and introduce a multivariate Normal variational distribution $q(\mathbf{u})$. We parameterize the covariance matrix of $q(\mathbf{u})$ with a cholesky factor \mathbf{L} . For the variational distribution over \mathbf{f} we choose the prior $p(\mathbf{f} | \mathbf{u}, \mathbf{X}, \mathbf{Z})$ so that the variational distribution over (\mathbf{f}, \mathbf{u}) is $p(\mathbf{f} | \mathbf{u}, \mathbf{X}, \mathbf{Z}) q(\mathbf{u})$. By introducing the auxiliary variable \mathbf{u} we obtain a variational objective that supports data subsampling, thus allowing us to scale to large datasets. Before we discuss applying sparse methods to any particular model in Sec. 3, we first take a step back and discuss variational inference for models with Normal likelihoods.

4.2 Variational Inference for Normal Likelihoods

We consider a regression model whose marginal likelihood is given by

$$p(\mathbf{Y} | \mathbf{X}) = \int d\mathbf{W} p(\mathbf{W}) \prod_{i=1}^N \mathcal{N}(\mathbf{y}_i | \Phi(\mathbf{x}_i, \mathbf{W}), \beta) \quad (9)$$

⁹Unless noted otherwise, if there are multiple GPs we share the inducing points.

where $\Phi(\mathbf{x}, \mathbf{W})$ is an arbitrary regressor function and \mathbf{W} denotes all the latent variables in the model. Note that all the models in Sec. 3.1 can be expressed in this form.¹⁰ Introducing a variational distribution $q(\mathbf{W})$ the variational objective—i.e. the evidence lower bound (ELBO)—can be written as

$$\text{ELBO} = \underbrace{\mathbb{E}_{q(\mathbf{W})} [\log p(\mathbf{Y}|\mathbf{X}, \mathbf{W})]}_{\text{ELL}} - \text{KL}(q(\mathbf{W})||p(\mathbf{W}))$$

where the first term is the expected log likelihood. We henceforth assume that the KL term is analytically tractable—as is the case for all the models we consider—and focus on the expected log likelihood (ELL). At this point there are two possibilities: i) we approximate the ELL with Monte Carlo samples; or ii) we compute the ELL analytically. As we will make use of both approaches in our experiments, let us consider each possibility in turn.

4.2.1 Stochastic Gradient Variational Bayes

For all the models in Sec. 3 we choose exclusively Normal variational distributions, which are amenable to the ‘reparameterization trick’ (Price, 1958; Kingma and Welling, 2013; Rezende et al., 2014). Consequently we can maximize the ELBO using stochastic gradient methods. At high level each iteration of training proceeds as follows:

1. subsample a mini-batch of data $(\mathbf{X}_{\text{mb}}, \mathbf{Y}_{\text{mb}})$
2. form the variational distribution $q(\mathbf{f}_{\text{mb}}) \equiv \int d\mathbf{u} p(\mathbf{f}_{\text{mb}}|\mathbf{u}, \mathbf{X}_{\text{mb}}, \mathbf{Z}) q(\mathbf{u})$
3. sample $\mathbf{f}_{\text{mb}} \sim q(\mathbf{f}_{\text{mb}})$ and compute a MC estimate of the expected log likelihood $\text{ELL}_{\text{mb}} = \mathbb{E}_{q(\mathbf{f}_{\text{mb}})} \log p(\mathbf{Y}_{\text{mb}}|\mathbf{f}_{\text{mb}})$
4. rescale ELL_{mb} to account for data subsampling
5. compute gradients of the ELBO with respect to model and variational parameters and take a gradient step

We refer the reader to (Salimbeni and Deisenroth, 2017) for an application of stochastic gradient methods to the particular case of deep GPs.

4.2.2 Analytic ELBOs

For all the models in Sec. 3.1 apart from the deep Gaussian process models the expected log likelihood can either be computed analytically or—for those models with

¹⁰For example, for the MOGP in Eqn. 1 \mathbf{W} correspond to the L latent function values $\{\mathbf{f}_\ell\} = \{\mathbf{F}_i\}$ and the latent matrix \mathbf{M} and $\Phi(\mathbf{x}, \mathbf{W}) = \mathbf{M}\mathbf{F}(\mathbf{x})$.

a non-linearity σ —almost analytically for a large class of non-linearities σ . Here by ‘almost’ analytically we mean that everything can be computed analytically up to one-dimensional quadrature. We include a brief summary of this approach and refer the reader to the supplementary materials for details.

The expected log likelihood for a single datapoint i can be rewritten as

$$\begin{aligned} \text{ELL}(i) &= \mathbb{E}_{q(\mathbf{W})} [\log p(y_i|\mathbf{X}, \mathbf{W})] \\ &= \frac{1}{2} \sum_{k=1}^{D_Y} \log \frac{\beta_k}{2\pi} - \sum_{k=1}^{D_Y} \frac{\beta_k}{2} \{ (y_{i,k} - m(\mathbf{x}_i)_k)^2 + v(\mathbf{x}_i)_k \} \end{aligned} \quad (10)$$

where the D_Y -dimensional mean and variance functions $\mathbf{m}(\mathbf{x})$ and $\mathbf{v}(\mathbf{x})$ are defined as

$$\begin{aligned} m(\mathbf{x})_k &= \mathbb{E}_{q(\mathbf{W})} [\Phi(\mathbf{x}, \mathbf{W})_k] \\ v(\mathbf{x})_k &= \mathbb{E}_{q(\mathbf{W})} [(\Phi(\mathbf{x}, \mathbf{W})_k - m(\mathbf{x})_k)^2] \end{aligned} \quad (11)$$

For the MOGP and GPRN in Sec. 3.1.1-3.1.2 as well as the SBGPRN in Sec. 3.1.4 both of these quantities can be computed analytically. For the N-MOGP and N-SBGPRN in Sec. 3.1.5-3.1.6 the mean function $\mathbf{m}(\mathbf{x})$ can be computed analytically for a wide class of non-linearities that includes, e.g., ReLU and the error function (erf).¹¹ Note that this implies that all of these models admit *analytic* predictive means. For this same class of non-linearities the variance function $\mathbf{v}(\mathbf{x})$ can be reduced to $\mathcal{O}(D_H^2)$ univariate Gaussian integrals, each of which can be efficiently computed using Gauss-Hermite quadrature; see the supplementary materials for details.

Inference for the Neural MOGP

To make the proceeding overview more concrete, we provide a more detailed discussion of inference for the Neural MOGP in 3.1.5, focusing on the case where the expected log likelihood is computed analytically.

We place a diagonal Normal variational distribution $q(\mathbf{M}) = \mathcal{N}(\mathbf{M}|\mathbf{M}_0, \sigma_{\mathbf{M}})$ on \mathbf{M} . We form L multivariate Normal variational distributions $\{q(\mathbf{u}_\ell)\}$ for the corresponding L GPs. Assuming we have analytic control over the non-linearity σ , we compute the mean function $\mathbf{m}(\mathbf{x})$:

$$\begin{aligned} m(\mathbf{x}_i)_k &= \mathbb{E}_{q(\mathbf{M}) \prod_\ell q(f_{\ell,i})} \left[(\mathbf{M}\sigma(\widetilde{\mathbf{M}}\mathbf{F}(\mathbf{x}_i)))_k \right] \\ &= \sum_h M_{0,kh} \mathbb{E}_{\prod_\ell q(f_{\ell,i})} \left[(\sigma(\widetilde{\mathbf{M}}\mathbf{F}(\mathbf{x}_i)))_h \right] \\ &= \sum_h M_{0,kh} m_h^\sigma(\mathbf{x}_i) \end{aligned} \quad (12)$$

¹¹More broadly, it includes all piecewise polynomial non-linearities as well as non-linearities of the form $\sigma(x) = \text{poly}(x)\text{erf}(x)$, where $\text{poly}(x)$ is polynomial.

Here $q(f_{\ell,i}) = \int d\mathbf{u}_\ell p(f_{\ell,i}|\mathbf{u}_\ell, \mathbf{x}_i, \mathbf{Z})q(\mathbf{u}_\ell)$ and we have implicitly introduced the mean activation function $\mathbf{m}^\sigma(\mathbf{x})$ on the last line. This quantity can be computed analytically as a function of $\widetilde{\mathbf{M}}$ and the means and variances of the marginal (Normal) distributions $\{q(f_{\ell,i})\}$; see the supplementary materials for details. Similarly we compute the variance function $\mathbf{v}(\mathbf{x})$:

$$\begin{aligned} \mathbf{v}(\mathbf{x}) &= \mathbf{v}_1(\mathbf{x}) + \mathbf{v}_2(\mathbf{x}) + \mathbf{v}_3(\mathbf{x}) \quad \text{with} \\ \mathbf{v}_1(\mathbf{x})_k &\equiv \sum_h \sum_{h'} M_{0,kh} v_{hh'}^\sigma(\mathbf{x}) M_{0,kh'} \\ \mathbf{v}_2(\mathbf{x})_k &\equiv \sum_h \sigma_{\mathbf{M},kh}^2 m_h^\sigma(\mathbf{x})^2 \\ \mathbf{v}_3(\mathbf{x})_k &\equiv \sum_h \sigma_{\mathbf{M},kh}^2 v_{hh}^\sigma(\mathbf{x}) \end{aligned} \quad (13)$$

Here $\mathbf{v}^\sigma(\mathbf{x})$ is the $D_H \times D_H$ covariance matrix corresponding to $\mathbf{m}^\sigma(\mathbf{x})$. This quantity can be computed efficiently using univariate quadrature, at a cost that scales quadratically in the number of hidden units D_H ; see the supplementary materials for details.

4.3 Variational Inference for Models with Latent Inputs

Inference for the models in Sec. 3.2 proceeds analogously to the models in Sec. 3.1, with the difference that we now need to infer the latent inputs \mathbf{X} . We introduce a factorized variational distribution $q(\mathbf{X}) = \prod_{i=1}^N q_i(\mathbf{x}_i)$, where each $q_i(\mathbf{x}_i)$ is a Normal distribution with a diagonal covariance matrix. During training we sample a mini-batch of latent inputs $\mathbf{X}_{\text{mb}} \sim q(\mathbf{X}_{\text{mb}})$ and make use of the reparameterization trick to compute gradients with respect to the variational parameters for the latent inputs. Since we do not make use of an amortized variational distribution for the local latent variables $\{\mathbf{x}_i\}$, at test time we need to fit a variational distribution $q(\mathbf{X}^*)$ corresponding to test data \mathbf{Y}^* . For more details on the inference procedure, see the supplementary details.

4.4 Fast Variational Inference for Sparse GPs

The primary bottleneck for the inference procedures outlined above arises from dealing with the (potentially) large number of Gaussian processes. In particular, some of the most expensive subcomputations involved in computing the variational objective include:

1. computing KL divergences $\text{KL}(q(\mathbf{u}_\ell)|p(\mathbf{u}_\ell))$
2. sampling from $q(\mathbf{f}_\ell)$ when doing inference via SGVB as in Sec. 4.2.1
3. computing the means and variances of the marginal distributions $q(f_{\ell,i})$ as required to compute analytic expected log likelihoods, c.f. Sec. 4.2.2

For this reason we leverage modern conjugate gradient methods as implemented in GPyTorch (Gardner et al.,

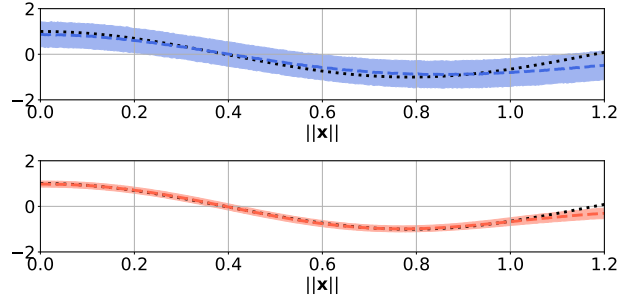


Figure 1: Predictions for the MOGP (top) and N-MOGP (bottom) for the synthetic regression experiment in Sec. 5.1. We depict the true function with a black dotted line, the mean model predictions with dashed lines, and colored uncertainty bands that extend from the 10th to the 90th percentile. Note that predictions for $\|\mathbf{x}\| > 1$ are extrapolations.

2018), which reduce the computational costs of 1-3 above from $O(N_{\text{ind}}^3)$ to $O(N_{\text{ind}}^2)$.

5 Experiments

In this section we conduct a series of experiments to illustrate the modeling potential of the models described in Sec. 3. First, in Sec. 5.1 we conduct a simple experiment with synthetic data. Next, in Sec. 5.2 we describe the robotics data that we use in all our remaining experiments. In Sec. 5.3 we consider regression models, while in Sec. 5.4 we consider the unsupervised setting. In addition in Sec. 5.5 we consider the effect of varying the number of ‘hidden units’ in the neural likelihood, while in Sec. 5.6-5.7 we examine the small data regime and missing outputs, respectively. All our experiments are implemented using GPyTorch (Gardner et al., 2018) and PyTorch (Paszke et al., 2017).

5.1 Synthetic Regression Experiment

We conduct a simple experiment using synthetic data to explore the modeling capacity of neural likelihoods. We consider the function $g : \mathbb{R}^5 \rightarrow \mathbb{R}^8$ given by $g_k(\mathbf{x}) = \cos(4\|\mathbf{x}\|)$ for $k = 1, \dots, 8$ where $\|\mathbf{x}\|$ is the L2-norm of \mathbf{x} . We sample $N = 1000$ inputs $\{\mathbf{x}_i\}$ from the unit ball in \mathbb{R}^5 and generate a dataset with noisy outputs via $\mathcal{D} = \{(\mathbf{x}_i, g(\mathbf{x}_i) + \sigma_0 \epsilon_i)\}$ with $\epsilon_i \sim \mathcal{N}(\mathbf{0}, \mathbf{1})$ and where $\sigma_0 = 0.1$. We then compare the quality of fit obtained by a MOGP versus a Neural MOGP. For both models we set the number of GPs to $L = 3$, use $N_{\text{ind}} = 200$ inducing points, and choose $D_H = 8$ for the N-MOGP.

To assess the quality of the fit visually, we choose a random line segment in \mathbb{R}^5 originating at the origin as

well as a random output dimension $k \in [1, 8]$ and depict model predictions $y_k(\mathbf{x}^*)$ along the line segment, see Fig. 1. While both models are able to learn reasonable mean functions, the MOGP exhibits a higher test MRMSE (0.166) than the N-MOGP (0.102). More strikingly, the N-MOGP is able to learn better calibrated uncertainties and thus obtains a substantially higher test log likelihood: 6.92 versus -0.72. One reason for this difference may be due to our choice of a bounded¹² non-linearity $\sigma(\cdot)$, which gives the N-MOGP more flexibility in learning a suitable variance function.¹³

5.2 Data

We use five robotics datasets for our main set of experiments, four of which were collected from real-world robots and one of which was generated using the MuJoCo physics simulator (Todorov et al., 2012). These datasets have been used in a number of papers, including references (Vijayakumar and Schaal, 2000; Meier et al., 2014; Cheng and Boots, 2017). In all five datasets the input and output dimensions correspond to various joint positions/velocities/etc. of the robot. These datasets form a good testbed for our proposed models, since the complex dynamics recorded in these data is highly non-linear and inherently multi-dimensional. See Table 1 for a summary of the different datasets.

Dataset	N_{train}	N_{test}	D_X	D_Y
R-Baxter	6918	2000	21	7
F-Baxter	14295	5000	21	14
Kuka	15068	5000	21	14
Sarcos	43933	5000	21	7
MuJoCo	10^5	10^4	23	9

Table 1: Datasets used in our experiments.

5.3 Regression

In this section we compare the performance of the various regression models defined in Sec. 3.1. To facilitate a fair comparison we choose the same number of GPs L in all models. In particular we choose $L = \lceil D_Y/2 \rceil$, where $\lceil \cdot \rceil$ denotes the ceiling function. For the (N-)DGP models we choose $L' = \lceil \frac{3}{4}D_Y \rceil$ so that the DGP prior is expected to be quite flexible. For the N-MOGP, N-SBGPRN, and N-DGP models, each of which includes a

¹²Specifically we chose the (shifted) error function $\sigma(x) = \text{erf}(x) + 1$.

¹³Recall from Eqn. 10 that in order for a regression model to obtain a large expected log likelihood it must learn a high-quality mean function *and* a high-quality variance function.

¹⁴MRMSE is the RMSE along each output dimension averaged across all output dimensions.

hyperparameter controlling the number of hidden units, we set $D_H = 2D_Y$, $D_H = D_Y$, and $D_H = 2D_Y$, respectively. For several of the models we also report results with a deep kernel (denoted by ‘DK’). For the models with neural likelihoods, we experiment with the following set of non-linearities $\sigma(\cdot)$:

1. ReLU: $\text{relu}(x) \equiv \max(0, x)$
2. Leaky ReLU: $\text{leaky}(x) \equiv \max(\epsilon x, x)$ with¹⁵ $\epsilon > 0$
3. Error function: $\text{erf}(x)$
4. Shifted error function: $\text{sherf}(x) \equiv 1 + \text{erf}(x)$

For a partial set of results see Table 2, which is organized to facilitate comparison between baseline models and their neural counterparts (e.g. MOGP versus N-MOGP). For additional details on the models and for additional results see the supplementary materials.

For most of the models and datasets predictive performance improves substantially with the addition of a neural likelihood; this is especially pronounced for the N-MOGP and (N-)SBGPRN. For the flexible DGP prior the gain in performance tends to be smaller (although see the R-Baxter and F-Baxter datasets). This smaller gain in performance, however, is largely a result of our choice of L' . Indeed if we choose $L = L'$ (so that the DGP prior is less powerful) the performance jump from DGP to N-DGP is substantial; see the supplementary materials. Note that in one case (F-Baxter) the N-MOGP has better predictive performance than the DGP and in three out of five datasets N-MOGP outperforms the GPRN in log likelihood, even though the GPRN achieves higher LLs than the MOGP on all five datasets. The N-SBGPRN and DK-N-SBGPRN perform particularly well across all five datasets; this is encouraging because we found these models easy and fast to train. Note as well that with the DK-N-SBGPRN we demonstrate that neural likelihoods can be successfully combined with deep kernels.

5.4 Unsupervised Learning

In this section we compare the performance of several unsupervised models defined by the general recipe in Sec. 3.2. In particular we consider unsupervised versions of the following models: MOGP, N-MOGP, and N-SBGPRN. We also trained unsupervised versions of the GPRN, DPG, and SBGPRN, but we do not report any results, since we found these models to perform poorly.¹⁶

¹⁵We choose $\epsilon = 0.35$ in our experiments.

¹⁶In order to get a deep GP with latent inputs to achieve good performance we would presumably need to implement a custom inference procedure more along the lines of the one used in (Dai et al., 2015). The sampling-based approach we used

Model	Dataset									
	R-Baxter		F-Baxter		Kuka		Sarcos		MuJoCo	
	LL	MRMSE	LL	MRMSE	LL	MRMSE	LL	MRMSE	LL	MRMSE
Baseline Models										
MOGP	1.38±0.18	0.297±0.007	13.16±0.46	0.285±0.004	15.64±0.40	0.174±0.006	1.63±0.04	0.250±0.001	-3.39±0.05	0.388±0.003
DK-MOGP	1.46±0.14	0.294±0.005	14.02±0.80	0.290±0.007	16.32±1.06	0.177±0.007	1.76±0.05	0.250±0.002	-1.97±0.13	0.347±0.004
GPRN	3.80±0.22	0.144±0.007	23.74±0.79	0.042±0.002	17.57±0.64	0.091±0.002	4.79±0.05	0.125±0.001	-2.50±0.11	0.336±0.004
DK-GPRN	2.78±0.38	0.179±0.009	24.77±0.79	0.040±0.001	19.14±0.64	0.089±0.002	4.52±0.11	0.133±0.003	-1.83±0.35	0.315±0.011
DGP	6.34±0.12	0.200±0.004	23.81±0.31	0.083±0.001	25.08±0.22	0.089±0.001	3.45±0.11	0.166±0.003	-2.46±0.16	0.354±0.013
Neural Likelihood Models										
N-MOGP	4.83±0.22	0.186±0.018	25.50±0.24	0.068±0.001	25.32±0.26	0.095±0.002	2.43±0.21	0.194±0.011	-3.06±0.17	0.383±0.014
SBGPRN	6.94±0.37	0.116±0.006	33.73±0.36	0.040±0.001	29.65±0.55	0.087±0.001	5.78±0.05	0.113±0.001	0.96±0.07	0.231±0.002
N-SBGPRN	7.55±0.18	0.105±0.002	35.23±0.33	0.039±0.001	31.19±0.33	0.087±0.001	6.02±0.07	0.109±0.001	1.54±0.08	0.219±0.002
DK-N-SBGPRN	7.80±0.14	0.107±0.003	36.01±0.34	0.038±0.001	31.58±0.39	0.086±0.001	6.14±0.09	0.107±0.001	1.87±0.12	0.212±0.003
N-DGP	7.30±0.23	0.110±0.004	27.36±0.42	0.057±0.002	25.41±0.37	0.088±0.001	3.69±0.07	0.158±0.003	-2.41±0.15	0.348±0.009

Table 2: Results for the regression experiments in Sec. 5.3. We report test log likelihoods per datapoint (LL) and mean root mean squared errors¹⁴(MRMSE) averaged over ten random train/test splits of the data. See the supplementary materials for additional results and model details.

Model	Dataset									
	R-Baxter		F-Baxter		Kuka		Sarcos		MuJoCo	
	LL	MRMSE	LL	MRMSE	LL	MRMSE	LL	MRMSE	LL	MRMSE
MOGP	-18.29±2.75	0.555±0.007	-34.93±10.12	0.583±0.015	-19.22±11.37	0.416±0.012	-32.58±6.48	0.654±0.011	-40.09±4.16	0.748±0.009
N-MOGP	-12.72±2.45	0.461±0.011	-18.88±5.10	0.402±0.025	-11.52±5.78	0.301±0.017	-24.43±2.17	0.500±0.018	-32.94±2.05	0.626±0.018
N-SBGPRN	2.45±1.19	0.355±0.005	19.49±6.64	0.094±0.008	22.82±1.89	0.100±0.006	-5.50±1.81	0.257±0.014	-18.06±0.57	0.408±0.007

Table 3: Results for the unsupervised learning experiments in Sec. 5.4. We report test log likelihoods per datapoint (LL) and mean root mean squared errors (MRMSE) averaged over ten random train/test splits of the data. See the supplementary materials for additional results and model details.

Note that we turn the supervised datasets described in Sec. 5.2 into unsupervised datasets by concatenating the inputs and outputs: $\mathbf{y}_i \leftarrow (\mathbf{x}_i, \mathbf{y}_i)$.

For all models we set the latent dimension to $D_X = 4$ and the number of GPs to $L = 4$. For the N-MOGP and N-SBGPRN we set $D_H = 14$ and $D_H = 7$, respectively. For a partial set of results see Table 3. For additional details on the models and for additional results see the supplementary materials.

Analogous to the regression models in the previous section, we find that the models with neural likelihoods substantially outperform the baseline MOGP. The performance gain is especially striking for the N-SBGPRN, which is the clear winner on all five datasets. This result is somewhat surprising, in that one might worry that the N-SBGPRN—which employs a deterministic neural network to mix the latent Gaussian processes in the

likelihood—could be especially susceptible to overfitting in the unsupervised setting. In fact, while we do see evidence¹⁷ of moderate overfitting on these datasets, we find that the increased flexibility of the likelihood easily compensates for any loss in performance caused by overfitting. This result is encouraging because (as above) we generally found the N-SBGPRN easy and fast to train.

5.5 Varying the Number of Hidden Units

To explore the effect of varying the number of hidden units D_H we train N-MOGP, N-SBGPRN, and N-DGP regression models on the Kuka and R-Baxter datasets for a range of $D_H \in [4, 20]$. See Fig. 2 for the results. As we would expect, we find that the performance—both in terms of the test log likelihood and the test MRMSE—tends to improve for all three models as we increase the number of hidden units. However, the effect is much

struggled to learn anything, probably at least in part due to high variance gradients.

¹⁷We typically find a difference of about 1 nat between train and test log likelihoods (here normalized per output dimension).

more pronounced for the N-MOGP and N-DGP, where the likelihoods are not as flexible as in the N-SBGPRN, which includes a (deterministic) neural network as a sub-component. Notably, as we increase the number of hidden units in the N-MOGP and N-DGP we close the majority or all of the performance gap between these two models and the N-SBGPRN. This is encouraging, since we expect the N-MOGP and N-DGP to be less prone to overfitting.

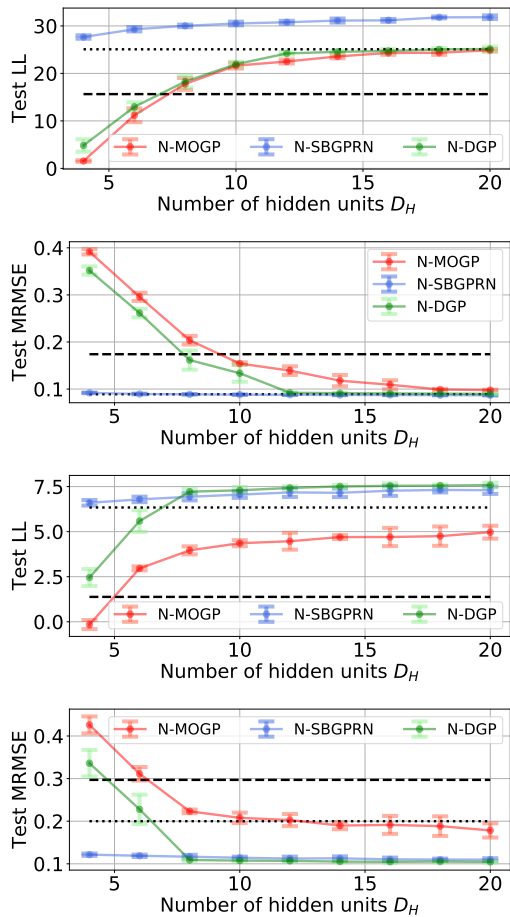


Figure 2: Test LLs and MRMSEs as a function of the number of hidden units on the Kuka (top) and R-Baxter (bottom) datasets for three neural GP models. For comparison we include results for the MOGP (dashed line) and DGP (dotted line). Results are averaged over ten random train/test splits.

5.6 Small Data Regime

Here we explore the extent to which the models defined in Sec. 3.1 are susceptible to overfitting. Among the models with neural likelihoods, we choose the N-MOGP, since, as discussed above, we expect it to be robust in the

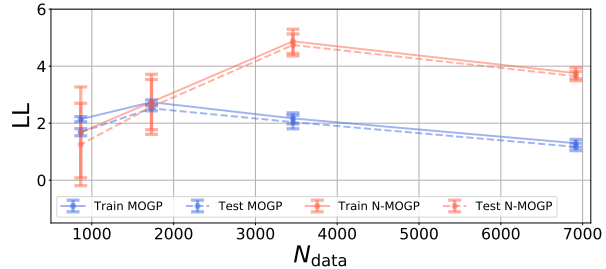


Figure 3: Training and Test LLs for models trained on varying amounts of training data N_{data} for the R-Baxter dataset. Results are averaged over fifteen random train/test splits for each value of N_{data} .

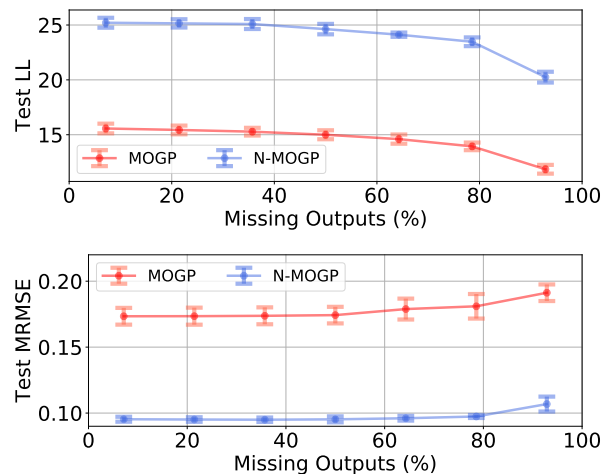


Figure 4: Test LLs (top) and MRMSEs (bottom) for the MOGP and N-MOGP trained with varying amounts of missing outputs $\{y_i\}$ for the Kuka dataset. Results are averaged over ten random train/test splits. See Sec. 5.7 for details.

small data regime.¹⁸ We then compare the N-MOGP to the MOGP and depict train and test log likelihoods obtained on the R-Baxter dataset as we vary the amount of training data, see Fig. 3. Although, as expected, we tend to observe lower log likelihoods as the number of training datapoints decreases, there is no evidence for overfitting. We observe similar results for an analogous experiment performed with the N-DGP. We thus expect the N-MOGP and the N-DGP to retain the (relative) robustness against overfitting that is characteristic of Gaussian process models.

5.7 Missing Outputs

Here we explore the extent to which the models defined in Sec. 3.1 can handle missing data. In particular we consider the case of missing outputs (i.e. each output \mathbf{y}_i has some number of output dimensions missing). We compare the N-MOGP to the MOGP and report test log likelihoods and MRMSEs obtained with the Kuka dataset as we vary the number of missing output dimensions, see Fig. 4. We find that, as is characteristic of Gaussian process models, both models maintain good performance in the presence of missing outputs. Moreover, the N-MOGP maintains its considerable performance advantage over the MOGP over the entire percentage range of missing outputs. See the supplementary materials for similar results obtained with the F-Baxter dataset.

6 Discussion

Neural likelihoods offer a simple and effective way to augment multi-output GP models and make them more flexible. We expect this class of likelihoods to be most useful in scenarios where the output dimension D_Y is large. In these cases it may be impractical to consider models constructed with $L = D_Y$ Gaussian processes so that it becomes necessary to choose $L \ll D_Y$. In order to form a likelihood, we then need to transform the L -dimensional latent vector of function values $\mathbf{F}(\mathbf{x})$ into D_Y dimensions. While this can be done with a simple linear transformation, as is done in the MOGP in Sec. 3.1.1, it is natural to consider more flexible alternatives as represented by the N-MOGP and SBGPRN. Empirically, we have seen that this added flexibility can result in substantial gains in predictive performance. Importantly, this added flexibility comes at little additional computational cost, as any computations done in the likelihood tend to be negligible when compared to the costs associated with the Gaussian process prior. Moreover, neural likelihoods are complementary to other methods for making GP priors flexible, as we demonstrated empirically in Sec. 5 by combining our approach with both deep GPs and deep kernels.

There are several interesting avenues for future research. In our experiments we have focused on regression and unsupervised learning. However, it could be of particular interest to apply neural likelihoods to the multi-task setting—for example to tasks that do not share a common set of inputs—where the additional flexibility offered by a neural likelihood could be especially beneficial. Finally, for the deterministic neural network used to de-

fine the SBGPRN in Sec. 3.1.4, we have relied on weight decay for regularization. It could be fruitful to explore variants of the SBGPRN that employ other techniques for regularizing neural networks, including for example dropout (Srivastava et al., 2014).

Acknowledgements

We cordially thank Ching-An Cheng for providing some of the datasets we used in our experiments. MJ would like to thank Felipe Petroski Such for help with infrastructure for efficient distribution of experiments.

References

- Mauricio Alvarez and Neil D Lawrence. Sparse convolved gaussian processes for multi-output regression. In *Advances in neural information processing systems*, pages 57–64, 2009.
- Mauricio A Álvarez and Neil D Lawrence. Computationally efficient convolved multiple output gaussian processes. *Journal of Machine Learning Research*, 12 (May):1459–1500, 2011.
- Mauricio A Alvarez, Lorenzo Rosasco, Neil D Lawrence, et al. Kernels for vector-valued functions: A review. *Foundations and Trends® in Machine Learning*, 4(3):195–266, 2012.
- Charles Blundell, Julien Cornebise, Koray Kavukcuoglu, and Daan Wierstra. Weight uncertainty in neural networks. *arXiv preprint arXiv:1505.05424*, 2015.
- Edwin V Bonilla, Kian M Chai, and Christopher Williams. Multi-task gaussian process prediction. In *Advances in neural information processing systems*, pages 153–160, 2008.
- Roberto Calandra, Jan Peters, Carl Edward Rasmussen, and Marc Peter Deisenroth. Manifold gaussian processes for regression. In *2016 International Joint Conference on Neural Networks (IJCNN)*, pages 3338–3345. IEEE, 2016.
- Ching-An Cheng and Byron Boots. Variational inference for gaussian process models with linear complexity. In *Advances in Neural Information Processing Systems*, pages 5184–5194, 2017.
- Kurt Cutajar, Edwin V Bonilla, Pietro Michiardi, and Maurizio Filippone. Random feature expansions for deep gaussian processes. In *Proceedings of the 34th International Conference on Machine Learning—Volume 70*, pages 884–893. JMLR. org, 2017.
- Zhenwen Dai, Andreas Damianou, Javier González, and Neil Lawrence. Variational auto-encoded deep gaussian processes. *arXiv preprint arXiv:1511.06455*, 2015.

¹⁸In addition we find that the SBGPRN and (N-)SBGPRN are actually susceptible to *underfitting* in this regime because of a tendency to get stuck in bad local minima.

- Andreas Damianou and Neil Lawrence. Deep gaussian processes. In *Artificial Intelligence and Statistics*, pages 207–215, 2013.
- Amir Dezfouli and Edwin V Bonilla. Scalable inference for gaussian process models with black-box likelihoods. In *Advances in Neural Information Processing Systems*, pages 1414–1422, 2015.
- Jacob Gardner, Geoff Pleiss, Kilian Q Weinberger, David Bindel, and Andrew G Wilson. Gpytorch: Blackbox matrix-matrix gaussian process inference with gpu acceleration. In *Advances in Neural Information Processing Systems*, pages 7587–7597, 2018.
- Marta Garnelo, Dan Rosenbaum, Chris J Maddison, Tiago Ramalho, David Saxton, Murray Shanahan, Yee Whye Teh, Danilo J Rezende, and SM Eslami. Conditional neural processes. *arXiv preprint arXiv:1807.01613*, 2018a.
- Marta Garnelo, Jonathan Schwarz, Dan Rosenbaum, Fabio Viola, Danilo J Rezende, SM Eslami, and Yee Whye Teh. Neural processes. *arXiv preprint arXiv:1807.01622*, 2018b.
- Alex Graves. Practical variational inference for neural networks. In *Advances in neural information processing systems*, pages 2348–2356, 2011.
- James Hensman, Nicolo Fusi, and Neil D Lawrence. Gaussian processes for big data. *arXiv preprint arXiv:1309.6835*, 2013.
- José Miguel Hernández-Lobato and Ryan Adams. Probabilistic backpropagation for scalable learning of bayesian neural networks. In *International Conference on Machine Learning*, pages 1861–1869, 2015.
- Wenbing Huang, Deli Zhao, Fuchun Sun, Huaping Liu, and Edward Chang. Scalable gaussian process regression using deep neural networks. In *Twenty-Fourth International Joint Conference on Artificial Intelligence*, 2015.
- Martin Jankowiak. Closed form variational objectives for bayesian neural networks with a single hidden layer. *arXiv preprint arXiv:1811.00686*, 2018.
- Diederik P Kingma and Jimmy Ba. Adam: A method for stochastic optimization. *arXiv preprint arXiv:1412.6980*, 2014.
- Diederik P Kingma and Max Welling. Auto-encoding variational bayes. *arXiv preprint arXiv:1312.6114*, 2013.
- Miguel Lázaro-Gredilla. Bayesian warped gaussian processes. In *Advances in Neural Information Processing Systems*, pages 1619–1627, 2012.
- Chao Ma, Yingzhen Li, and José Miguel Hernández-Lobato. Variational implicit processes. *arXiv preprint arXiv:1806.02390*, 2018.
- César Lincoln C Mattos, Zhenwen Dai, Andreas Damianou, Jeremy Forth, Guilherme A Barreto, and Neil D Lawrence. Recurrent gaussian processes. *arXiv preprint arXiv:1511.06644*, 2015.
- Franziska Meier, Philipp Hennig, and Stefan Schaal. Incremental local gaussian regression. In *Advances in Neural Information Processing Systems*, pages 972–980, 2014.
- Edward W Ng and Murray Geller. A table of integrals of the error functions. *Journal of Research of the National Bureau of Standards B*, 73(1):1–20, 1969.
- Trung V Nguyen, Edwin V Bonilla, et al. Collaborative multi-output gaussian processes. In *UAI*, pages 643–652, 2014.
- Adam Paszke, Sam Gross, Soumith Chintala, Gregory Chanan, Edward Yang, Zachary DeVito, Zeming Lin, Alban Desmaison, Luca Antiga, and Adam Lerer. Automatic differentiation in pytorch. 2017.
- Robert Price. A useful theorem for nonlinear devices having gaussian inputs. *IRE Transactions on Information Theory*, 4(2):69–72, 1958.
- Carl Edward Rasmussen. Gaussian processes in machine learning. In *Summer School on Machine Learning*, pages 63–71. Springer, 2003.
- Danilo Jimenez Rezende, Shakir Mohamed, and Daan Wierstra. Stochastic backpropagation and approximate inference in deep generative models. *arXiv preprint arXiv:1401.4082*, 2014.
- Hugh Salimbeni and Marc Deisenroth. Doubly stochastic variational inference for deep gaussian processes. In *Advances in Neural Information Processing Systems*, pages 4588–4599, 2017.
- Matthias Seeger, Yee-Whye Teh, and Michael Jordan. Semiparametric latent factor models. Technical report, 2005.
- Edward Snelson, Zoubin Ghahramani, and Carl E Rasmussen. Warped gaussian processes. In *Advances in neural information processing systems*, pages 337–344, 2004.
- Nitish Srivastava, Geoffrey Hinton, Alex Krizhevsky, Ilya Sutskever, and Ruslan Salakhutdinov. Dropout: a simple way to prevent neural networks from overfitting. *The Journal of Machine Learning Research*, 15(1):1929–1958, 2014.
- Shengyang Sun, Guodong Zhang, Chaoqi Wang, Wenyuan Zeng, Jiaman Li, and Roger Grosse. Differentiable compositional kernel learning for gaussian processes. *arXiv preprint arXiv:1806.04326*, 2018.
- Kevin Swersky, Jasper Snoek, and Ryan P Adams. Multi-task bayesian optimization. In *Advances in neu-*

- ral information processing systems*, pages 2004–2012, 2013.
- Michalis Titsias. Variational learning of inducing variables in sparse gaussian processes. In *Artificial Intelligence and Statistics*, pages 567–574, 2009.
- Emanuel Todorov, Tom Erez, and Yuval Tassa. Mujoco: A physics engine for model-based control. In *2012 IEEE/RSJ International Conference on Intelligent Robots and Systems*, pages 5026–5033. IEEE, 2012.
- Sethu Vijayakumar and Stefan Schaal. Locally weighted projection regression: An $o(n)$ algorithm for incremental real time learning in high dimensional space. In *Proceedings of the Seventeenth International Conference on Machine Learning (ICML 2000)*, volume 1, pages 288–293, 2000.
- Christopher Williams, Stefan Klanke, Sethu Vijayakumar, and Kian M Chai. Multi-task gaussian process learning of robot inverse dynamics. In *Advances in Neural Information Processing Systems*, pages 265–272, 2009.
- Andrew Wilson and Ryan Adams. Gaussian process kernels for pattern discovery and extrapolation. In *International Conference on Machine Learning*, pages 1067–1075, 2013.
- Andrew Gordon Wilson, David A Knowles, and Zoubin Ghahramani. Gaussian process regression networks. *arXiv preprint arXiv:1110.4411*, 2011.
- Andrew Gordon Wilson, Zhiting Hu, Ruslan Salakhutdinov, and Eric P Xing. Deep kernel learning. In *Artificial Intelligence and Statistics*, pages 370–378, 2016.

7 Appendix

7.1 Additional Experimental Results

7.1.1 Regression

See Table 4 for additional results for the (N-)MOGP models. Here as elsewhere the prefix ‘DK’ indicates that the given model is equipped with a deep kernel.

See Table 5 for additional results for the GPRN family of models. Perhaps not surprisingly, the DK-N-SBGPRN, which contain neural networks in both the kernel and the likelihood, is the best performing model across the board.

See Table 6 for additional results for the (N-)DGP models. The models with $L' = L$ employ less flexible priors than the models for which we report results in the main text. Note that, as mentioned in the main text, the performance gain from adding neural likelihoods is significantly larger for these models.

7.1.2 Unsupervised Learning

See Table 7 for additional results for the unsupervised learning experiments in Sec. 5.4. For the N-MOGP models we consider both $D_H = 7$ and $D_H = 14$ hidden units.

7.2 Experimental Details

For all experiments we use the Adam optimizer (Kingma and Ba, 2014).

7.2.1 Synthetic Experiment

We follow the training protocol discussed in the next section.

7.2.2 Regression

We specify some of the details of our regression models and their corresponding inference procedures omitted in the main text. Our RBF kernels use separate length scales for each input dimension. For all models we choose $N_{\text{ind}} = 400$ inducing points, except for the GPRN (where we choose $N_{\text{ind}} = 100$) and for the N-DGP models (where we choose $N_{\text{ind}} = 400$ for the first layer of GPs and $N_{\text{ind}} = 100$ for the second layer of GPs). We find that these models can struggle to take advantage of more inducing points and become susceptible to getting stuck in bad local optima when the number of inducing points is too large. For the results in Table 2 we choose the shifted erf non-linearity for the N-MOGP, the

leaky ReLU non-linearity for the N-SBGPRN and DK-N-SBGPRN, and the erf non-linearity for the N-DGP.

We train all models for 250 epochs. We use mini-batch sizes of 1000, 500, 500, 500, and 250 for the MuJoCo, Kuka, F-Baxter, Sarcos, and R-Baxter datasets, respectively, except for the (N-)DGP models, where we double the mini-batch size. For each training/test split we use 5 random parameter initializations and only train the best performing model (in terms of training LL) to completion. Depending on the model we use initial learning rates in the range $[0.01, 0.05]$, which we reduce stepwise over the course of training. For some of the (N-)DGP models we also found it useful to employ KL annealing during the first 20 epochs of training. Except for the inducing points for the second layer of GPs in the DGP (which we initialize randomly and where we do not share the inducing points across the L' GPs), we initialize inducing points using k-means clustering on the training data inputs $\{\mathbf{x}_i\}$.

For uniformity we train all models except for the GPRN¹⁹ using the SGVB approach outlined in Sec. 4.2.1. That is, we compute stochastic gradient estimates of the expected log likelihood by drawing $N_{\text{samples}} = 250$ samples from the variational distributions $\{q_{\ell}(\mathbf{f}_{\text{mb}})\}$ for each GP. For the (N-)DGP models, where the nesting of multiple layers of Gaussian processes makes sampling particularly expensive, we instead use $N_{\text{samples}} = 5$ samples.²⁰ Note that for models that make use of a mixing matrix \mathbf{M} we simply integrate \mathbf{M} out and never sample \mathbf{M} .

Throughout we report test log likelihoods using an estimator of the form

$$\log p(\mathbf{Y}^*|\mathbf{X}^*) \approx \frac{1}{N_{\text{outer}}} \sum_{k=1}^{N_{\text{outer}}} \log \left(\frac{1}{N_{\text{inner}}} \sum_{j=1}^{N_{\text{inner}}} p(\mathbf{Y}^*|\mathbf{X}^*, \mathbf{F}_{jk}^*) \right)$$

where each sample \mathbf{F}_{jk}^* is from the relevant variational distribution and $N_{\text{outer}} = 25$ and $N_{\text{inner}} = 50$.

Bias in Hidden Units

For the N-MOGP, N-SBGPRN, and N-DGP we use D_H bias terms in the non-linearity σ that appears in the likelihood. That is, the expression $\sigma(\widehat{\mathbf{M}}\mathbf{F})$ in Eqn. 5 is in fact shorthand for $\sigma(\widehat{\mathbf{M}}\mathbf{F} + \mathbf{b})$, where \mathbf{b} is a D_H -dimensional vector of bias terms with a unit Normal prior. During inference, we use mean field Normal variational distributions for each bias term b_h . For these same models, because of the flexibility of the bias units, we use Gaus-

¹⁹We train the GPRN by computing analytic expected log likelihoods as outlined in Sec. 4.2.2.

²⁰Our inference procedure for the (N-)DGP models closely follows that of (Salimbeni and Deisenroth, 2017).

Model	Dataset									
	R-Baxter		F-Baxter		Kuka		Sarcos		MuJoCo	
	LL	MRMSE	LL	MRMSE	LL	MRMSE	LL	MRMSE	LL	MRMSE
MOGP	1.38±0.18	0.297±0.007	13.16±0.46	0.285±0.004	15.64±0.40	0.174±0.006	1.63±0.04	0.250±0.001	-3.39±0.05	0.388±0.003
DK-MOGP	1.46±0.14	0.294±0.005	14.02±0.80	0.290±0.007	16.32±1.06	0.177±0.007	1.76±0.05	0.250±0.002	-1.97±0.13	0.347±0.004
N-MOGP (erf)	4.59±0.55	0.183±0.028	18.37±0.77	0.128±0.016	22.90±0.43	0.112±0.006	2.11±0.25	0.218±0.015	-3.20±0.33	0.384±0.021
N-MOGP (relu)	0.88±1.76	0.365±0.089	18.53±0.61	0.103±0.011	21.64±0.79	0.107±0.007	1.99±0.10	0.220±0.007	-3.02±0.05	0.377±0.003
N-MOGP (sherp)	4.83±0.22	0.186±0.018	25.50±0.24	0.068±0.001	25.32±0.26	0.095±0.002	2.43±0.21	0.194±0.011	-3.06±0.17	0.383±0.014
N-MOGP (leaky)	4.80±0.34	0.174±0.016	23.00±0.50	0.075±0.002	23.50±0.48	0.097±0.002	2.16±0.15	0.212±0.008	-2.92±0.05	0.373±0.003

Table 4: Full results for the (N-)MOGP models in Sec. 5.3. We report test log likelihoods per datapoint (LL) and mean root mean squared errors (MRMSE) averaged over ten random train/test splits of the data.

Model	Dataset									
	R-Baxter		F-Baxter		Kuka		Sarcos		MuJoCo	
	LL	MRMSE	LL	MRMSE	LL	MRMSE	LL	MRMSE	LL	MRMSE
GPRN	3.80±0.22	0.144±0.007	23.74±0.79	0.042±0.002	17.57±0.64	0.091±0.002	4.79±0.05	0.125±0.001	-2.50±0.11	0.336±0.004
DK-GPRN	2.78±0.38	0.179±0.009	24.77±0.79	0.040±0.001	19.14±0.64	0.089±0.002	4.52±0.11	0.133±0.003	-1.83±0.35	0.315±0.011
SBGPRN	6.94±0.37	0.116±0.006	33.73±0.36	0.040±0.001	29.65±0.55	0.087±0.001	5.78±0.05	0.113±0.001	0.96±0.07	0.231±0.002
DK-SBGPRN	6.84±0.47	0.116±0.007	34.26±0.37	0.039±0.001	29.53±0.52	0.088±0.002	5.93±0.06	0.110±0.001	1.56±0.10	0.218±0.002
N-SBGPRN (erf)	7.47±0.26	0.105±0.004	34.59±0.33	0.042±0.001	29.83±0.63	0.088±0.001	5.80±0.07	0.113±0.001	1.06±0.10	0.231±0.003
N-SBGPRN (relu)	7.24±0.35	0.110±0.006	35.75±0.26	0.038±0.001	31.30±0.46	0.087±0.002	5.90±0.13	0.111±0.002	1.52±0.08	0.220±0.003
N-SBGPRN (sherp)	6.72±0.16	0.119±0.002	35.69±0.40	0.039±0.001	31.70±0.36	0.087±0.002	6.00±0.07	0.110±0.001	1.24±0.10	0.226±0.002
N-SBGPRN (leaky)	7.55±0.18	0.105±0.002	35.23±0.33	0.039±0.001	31.19±0.33	0.087±0.001	6.02±0.07	0.109±0.001	1.54±0.08	0.219±0.002
DK-N-SBGPRN (erf)	7.55±0.21	0.107±0.003	35.41±0.32	0.041±0.001	30.81±0.54	0.088±0.001	5.93±0.10	0.110±0.001	1.41±0.08	0.222±0.002
DK-N-SBGPRN (relu)	7.52±0.29	0.104±0.003	36.66±0.30	0.037±0.001	31.91±0.44	0.086±0.001	6.04±0.10	0.108±0.001	1.86±0.08	0.211±0.002
DK-N-SBGPRN (sherp)	6.66±0.40	0.118±0.008	36.24±0.36	0.038±0.001	32.30±0.48	0.086±0.001	6.13±0.06	0.107±0.001	1.60±0.10	0.217±0.003
DK-N-SBGPRN (leaky)	7.80±0.14	0.107±0.003	36.01±0.34	0.038±0.001	31.58±0.39	0.086±0.001	6.14±0.09	0.107±0.001	1.87±0.12	0.212±0.003

Table 5: Full results for the GPRN, SBGPRN, and N-SBGPRN models in Sec. 5.3. We report test log likelihoods per datapoint (LL) and mean root mean squared errors (MRMSE) averaged over ten random train/test splits of the data.

sian priors with (fixed) zero mean functions, while for all other Gaussian process priors we use (trainable) constant mean functions.

Deep Kernels

All our deep kernels make use of neural networks with two hidden layers, each with 50 hidden units, and have the same number of output dimensions as input dimensions. We use tanh non-linearities. We also use a multiplicative parameterization of the deep kernels such that at initialization each is close to the identity function.

SBGPRN Neural Networks

Throughout the neural network $M(\mathbf{x})$ that appears in the SBGPRN and N-SBGPRN has two hidden layers, each with 50 units, and utilizes tanh non-linearities.

7.2.3 Unsupervised Learning

We specify some of the details of our unsupervised models and their corresponding inference procedures omitted

in the main text. We use $N_{\text{ind}} = 200$ inducing points for all models. For the results in Table 3 we choose the leaky ReLU non-linearity for the N-MOGP and the ReLU non-linearity for the N-SBGPRN. The training procedure and modeling setup generally follows that of the regression models, with the important difference that (except for the latent inputs, which we always sample) we compute analytic expected log likelihoods as described in Sec. 4.2.2. We use $N_{\text{qp}} = 100$ quadrature points. During training we sample a single latent $\mathbf{x}_i \sim q(\mathbf{x}_i)$ for each datapoint. We find that using analytic ELBOs during training leads to better stability and performance. In contrast to the regression models, the RBF kernels in our unsupervised learning experiments use the same length scale for all dimensions. During test time, we introduce a new variational distribution $q(\mathbf{X}^*)$ for the unseen data and fit $q(\mathbf{X}^*)$ by maximizing the ELBO. That is, fitting $q(\mathbf{X}^*)$ proceeds analogously to training, except that now everything except for $q(\mathbf{X}^*)$ is kept fixed (i.e. the kernel hyperparameters, the variational distributions $q(\mathbf{u}_\ell)$, etc.). We initialize $q(\mathbf{X}^*)$ by using a nearest neighbor algorithm to find points in the training data that are close to points in

Model	Dataset									
	R-Baxter		F-Baxter		Kuka		Sarcos		MuJoCo	
	LL	MRMSE	LL	MRMSE	LL	MRMSE	LL	MRMSE	LL	MRMSE
DGP	6.34±0.12	0.200±0.004	23.81±0.31	0.083±0.001	25.08±0.22	0.089±0.001	3.45±0.11	0.166±0.003	-2.46±0.16	0.354±0.013
N-DGP (erf)	7.30±0.23	0.110±0.004	27.36±0.42	0.057±0.002	25.41±0.37	0.088±0.001	3.69±0.07	0.158±0.003	-2.41±0.15	0.348±0.009
N-DGP (sherf)	3.27±2.58	0.232±0.082	27.42±0.49	0.058±0.003	25.63±0.47	0.091±0.002	2.95±0.82	0.192±0.035	-2.41±0.12	0.357±0.009
N-DGP (leaky)	7.42±0.17	0.107±0.003	27.93±0.21	0.053±0.001	25.66±0.29	0.089±0.001	3.65±0.10	0.161±0.005	-2.99±0.96	0.390±0.052
DGP ($L' = L$)	2.91 ± 0.29	0.315 ± 0.029	12.89 ± 0.69	0.284 ± 0.005	15.60 ± 0.36	0.190 ± 0.007	2.31 ± 0.05	0.243 ± 0.002	-2.81 ± 0.16	0.384 ± 0.021
N-DGP ($L' = L$, erf)	5.98 ± 0.20	0.145 ± 0.017	21.77 ± 0.65	0.081 ± 0.005	23.69 ± 0.23	0.103 ± 0.004	2.82 ± 0.16	0.214 ± 0.010	-2.78 ± 0.14	0.388 ± 0.015
N-DGP ($L' = L$, sherf)	3.21 ± 2.51	0.238 ± 0.084	24.63 ± 0.97	0.068 ± 0.004	24.73 ± 0.46	0.093 ± 0.002	2.93 ± 0.21	0.201 ± 0.010	-2.68 ± 0.17	0.374 ± 0.018
N-DGP ($L' = L$, leaky)	5.83 ± 0.18	0.169 ± 0.016	24.43 ± 0.41	0.067 ± 0.001	24.61 ± 0.32	0.092 ± 0.001	2.97 ± 0.24	0.197 ± 0.012	-3.26 ± 0.54	0.405 ± 0.027

Table 6: Full results for the (N-)DGP models in Sec. 5.3. We report test log likelihoods per datapoint (LL) and mean root mean squared errors (MRMSE) averaged over ten random train/test splits of the data. Unless noted otherwise $L' = \lceil \frac{3}{4} D_Y \rceil$.

Model	Dataset									
	R-Baxter		F-Baxter		Kuka		Sarcos		MuJoCo	
	LL	MRMSE	LL	MRMSE	LL	MRMSE	LL	MRMSE	LL	MRMSE
MOGP	-18.29±2.75	0.555±0.007	-34.93±10.12	0.583±0.015	-19.22±11.37	0.416±0.012	-32.58±6.48	0.654±0.011	-40.09±4.16	0.748±0.009
N-MOGP ($D_H = 7$, erf)	-14.51±3.81	0.483±0.020	-25.87±4.43	0.506±0.022	-20.36±5.65	0.379±0.015	-27.80±2.52	0.634±0.042	-39.63±2.57	0.762±0.025
N-MOGP ($D_H = 7$, relu)	-30.60±3.41	0.782±0.061	-30.92±3.77	0.654±0.064	-20.73±5.90	0.504±0.088	-30.06±2.05	0.735±0.054	-36.53±1.14	0.765±0.029
N-MOGP ($D_H = 7$, sherf)	-13.98±3.14	0.500±0.035	-27.04±6.49	0.522±0.038	-23.59±12.63	0.388±0.024	-28.51±3.76	0.633±0.039	-42.71±6.23	0.768±0.033
N-MOGP ($D_H = 7$, leaky)	-13.45±1.78	0.489±0.021	-23.65±4.46	0.483±0.028	-17.00±9.57	0.373±0.027	-26.75±5.33	0.569±0.030	-35.40±2.26	0.691±0.015
N-MOGP ($D_H = 14$, erf)	-18.65±7.67	0.490±0.030	-20.00±4.69	0.428±0.028	-23.47±10.88	0.349±0.024	-24.08±2.62	0.536±0.034	-34.69±1.96	0.679±0.037
N-MOGP ($D_H = 14$, relu)	-26.91±3.42	0.726±0.064	-28.87±5.06	0.602±0.082	-18.33±5.13	0.479±0.086	-27.36±2.23	0.652±0.038	-32.32±0.88	0.670±0.021
N-MOGP ($D_H = 14$, sherf)	-15.87±6.49	0.461±0.016	-23.20±9.07	0.435±0.042	-28.77±16.68	0.363±0.028	-23.58±2.81	0.520±0.024	-35.62±1.99	0.679±0.035
N-MOGP ($D_H = 14$, leaky)	-12.72±2.45	0.461±0.011	-18.88±5.10	0.402±0.025	-11.52±5.78	0.301±0.017	-24.43±2.17	0.500±0.018	-32.94±2.05	0.626±0.018
N-SBGPRN (erf)	1.88±1.36	0.348±0.004	17.69±4.49	0.089±0.007	22.18±2.07	0.089±0.004	-7.74±3.63	0.259±0.021	-19.10±2.22	0.412±0.017
N-SBGPRN (relu)	2.45±1.19	0.355±0.005	19.49±6.64	0.094±0.008	22.82±1.89	0.100±0.006	-5.50±1.81	0.257±0.014	-18.06±0.57	0.408±0.007
N-SBGPRN (sherf)	-1.16±3.95	0.353±0.007	13.09±11.64	0.100±0.011	15.60±5.30	0.105±0.011	-9.63±5.32	0.263±0.027	-18.41±2.46	0.405±0.016
N-SBGPRN (leaky)	1.33±2.13	0.347±0.005	11.14±8.37	0.091±0.007	15.65±6.65	0.091±0.007	-9.44±3.26	0.258±0.016	-21.45±1.93	0.422±0.013

Table 7: Full results for the unsupervised learning experiments in Sec. 5.4. We report test log likelihoods per datapoint (LL) and mean root mean squared errors (MRMSE) averaged over ten random train/test splits of the data.

the test data; we then initialize the means of $q(\mathbf{x}_i^*)$ by using the mean of the variational distribution $q(\mathbf{x}_j)$ of the training datapoint \mathbf{x}_j that is closest to \mathbf{x}_i^* .

7.2.4 Varying D_H

The experimental protocol for these experiments closely follows that of the regression experiments in Sec. 5.3.

7.2.5 Small Data Regime

The experimental protocol for these experiments closely follows that of the regression experiments in Sec. 5.3, with the difference that we only use $N_{\text{ind}} = 250$ inducing points and that as we reduce the training set size we reduce the mini-batch size proportionally.

7.2.6 Missing Outputs

The experimental protocol for these experiments closely follows that of the regression experiments in Sec. 5.3.

For each missing output percentage the number of missing output dimensions for each output \mathbf{y}_i is identical (e.g. 3/14 output dimensions are missing). The particular missing output dimensions for each datapoint are different between each train/test split. For additional results obtained with the F-Baxter dataset see Fig. 5.

7.3 Expectations of Non-linearities

We discuss how we compute the expectations required to form analytic expected log likelihoods as described for the N-MOGP in Sec. 4.2.2. Here we focus on the error function non-linearity $g(x) = \text{erf}(x)$. An analytic expression for the mean function can be obtained from a table of integrals:²¹

$$\mathbb{E}_{\mathcal{N}(x|\mu,\sigma)}[\text{erf}(x)] = \text{erf}\left(\frac{\mu}{\sqrt{1+2\sigma^2}}\right) \quad (14)$$

²¹See e.g. the integrals listed in (Ng and Geller, 1969)

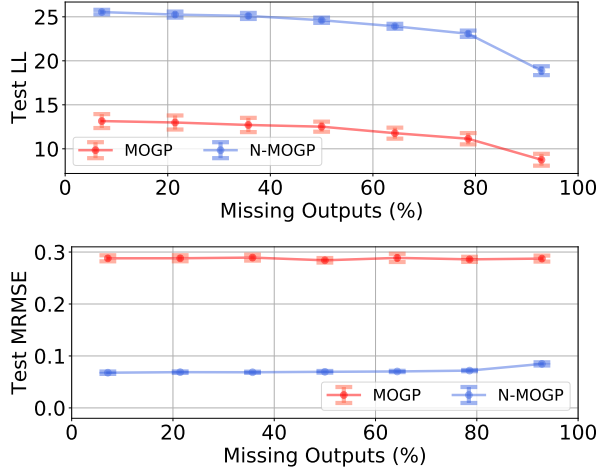


Figure 5: Test LLs (top) and MRMSEs (bottom) for the MOGP and N-MOGP trained with varying amounts of missing outputs $\{y_i\}$ for the F-Baxter dataset. Results are averaged over ten random train/test splits.

An analytic expression for the corresponding second moment is not readily available but can be computed efficiently using quadrature:

$$\begin{aligned}
\mathbb{E}_{\mathcal{N}(x|\mu,\sigma)} [\text{erf}(x)^2] &= \mathbb{E}_{\mathcal{N}(x|0,1/\sqrt{2})} [\text{erf}(\sqrt{2}\sigma x + \mu)^2] \\
&= \frac{1}{\sqrt{\pi}} \int dx e^{-x^2} \text{erf}(\sqrt{2}\sigma x + \mu)^2 \\
&\approx \frac{1}{\sqrt{\pi}} \sum_{i=1}^{N_q} w_i \text{erf}(\sqrt{2}\sigma x_i + \mu)^2
\end{aligned} \tag{15}$$

where $\{(x_i, w_i)\}$ are the sample points and weights from a Gauss-Hermite quadrature rule of order N_q (conventionally defined w.r.t. the weighting function e^{-x^2}). Finally, we would like to compute the bivariate expectation

$$\mathbb{E}_{\mathcal{N}(\mathbf{x}|\boldsymbol{\mu},\boldsymbol{\Sigma})} [g(x_1)g(x_2)] = \mathbb{E}_{\mathcal{N}(\mathbf{x}|\boldsymbol{\mu},\boldsymbol{\Sigma})} [\text{erf}(x_1)\text{erf}(x_2)] \tag{16}$$

An analytic expression is not readily available but we can do “half” of the integral analytically and compute the remaining univariate integral using quadrature. Changing variables so that the Normal distribution has a diagonal covariance matrix, we obtain:

$$\frac{1}{\sqrt{\pi}} \int dx_1 e^{-x_1^2} g(\sqrt{2}L_{11}x_1 + \mu_1)h(x_1) \tag{17}$$

where \mathbf{L} is the Cholesky decomposition²² of $\boldsymbol{\Sigma}$ with $\boldsymbol{\Sigma} = \mathbf{L}\mathbf{L}^T$ and $h(x_1)$ is given by the mean function

$$\begin{aligned}
h(x_1) &= \mathbb{E}_{\mathcal{N}(x_2|0,1/\sqrt{2})} [g(\sqrt{2}L_{21}x_1 + \sqrt{2}L_{22}x_2 + \mu_2)] \\
&= \mathbb{E}_{\mathcal{N}(\tilde{x}_2|\sqrt{2}L_{21}x_1 + \mu_2, L_{22})} [g(\tilde{x}_2)]
\end{aligned} \tag{18}$$

Consequently whenever an analytic expression is available for this inner expectation—as is the case for the error function, recall Eqn. 14—the bivariate expectation in Eqn. 16 can be efficiently computed with univariate Gauss-Hermite quadrature.

The identity Eqn. 14 can be manipulated to yield all expectations of the form $\mathbb{E}_{\mathcal{N}(x|\mu,\sigma)} [x^n \text{erf}(x)]$, thus making all the mean functions for all nonlinearities of the form $g(x) = \text{poly}(x)\text{erf}(x)$ for some polynomial $\text{poly}(x)$ analytically tractable. For example we have

$$\begin{aligned}
\mathbb{E}_{\mathcal{N}(x|\mu,\sigma)} [x \text{erf}(x)] &= \mu \text{erf}\left(\frac{\mu}{\sqrt{1+2\sigma^2}}\right) + \\
&\quad \frac{2\sigma^2}{\sqrt{\pi}(1+2\sigma^2)^{1/2}} e^{-\frac{\mu^2}{1+2\sigma^2}}
\end{aligned} \tag{19}$$

and

$$\begin{aligned}
\mathbb{E}_{\mathcal{N}(x|\mu,\sigma)} [x^2 \text{erf}(x)] &= (\mu^2 + \sigma^2) \text{erf}\left(\frac{\mu}{\sqrt{1+2\sigma^2}}\right) + \\
&\quad \frac{4\mu\sigma^2(1+\sigma^2)}{\sqrt{\pi}(1+2\sigma^2)^{3/2}} e^{-\frac{\mu^2}{1+2\sigma^2}}
\end{aligned} \tag{20}$$

For the analytic expressions needed to deal with piecewise polynomial non-linearities like ReLU we refer the reader to (Jankowiak, 2018).

Finally, note that above (e.g. in Eqn. 14) we have given analytic expressions for expectations with respect to 1-dimensional Normal random variables. However, in Sec. 4.2.2 the mean and variance functions for the activations, $\mathbf{m}^\sigma(\mathbf{x})$ and $\mathbf{v}^\sigma(\mathbf{x})$, are expressed as expectations with respect to the product distribution $\prod_\ell q(f_{\ell,i})$. Since, however, the argument of the non-linearity $\sigma(\cdot)$ in these equations (see e.g. Eqn. 12) is a linear combination of 1-dimensional Normal random variables, the argument is in fact a 1-dimensional Normal random variable, and so our analytic results are directly applicable. We simply appeal to the fact that if $a_i \sim \mathcal{N}(\mu_i, \sigma_i)$ and $x \equiv \sum_i b_i a_i$ for some constants $\{b_i\}$, then $x \sim \mathcal{N}(\mu, \sigma)$ with $\mu = \sum_i b_i \mu_i$ and $\sigma^2 = \sum_i b_i^2 \sigma_i^2$.

²²Since $\boldsymbol{\Sigma}$ is two-dimensional this decomposition is trivial to compute: $L_{11} = \sqrt{\Sigma_{11}}$, etc.